Chemistry–A European Journal
Research Article
doi.org/10.1002/chem.202302237
Chemistry Europe
European Chemical Societies Publishing
www.chemeurj.org

Special Collection

Exploring the Potential of Anthraquinone-Based Hybrids for Identifying a Novel Generation of Antagonists for the Smoothened Receptor in HH-Dependent Tumour

Deborah Quaglio[+],[a] Paola Infante[+],[b] Silvia Cammarone,[a] Lara Lamelza,[a] Marilisa Conenna,[b] Francesca Ghirga,*[a] Gennaro Adabbo,[b] Luca Pisano,[a] Lucia Di Marcotullio,*[b, c] Bruno Botta,[a] and Mattia Mori[d]

Natural products (NPs) are highly profitable pharmacological tools due to their chemical diversity and ability to modulate biological systems. Accessing new chemical entities while retaining the biological relevance of natural chemotypes is a fundamental goal in the design of novel bioactive compounds. Notably, NPs have played a crucial role in understanding Hedgehog (HH) signalling and its pharmacological modulation in anticancer therapy. However, HH antagonists developed so far have shown several limitations, thus growing interest in the design of second-generation HH inhibitors. Through smart manipulation of the NPs core-scaffold, unprecedented and intriguing architectures have been achieved following different design strategies. This study reports the rational design and synthesis of a first and second generation of anthraquinone-based hybrids by combining the rhein scaffold with variously substituted piperazine nuclei that are structurally similar to the active portion of known SMO antagonists, the main transducer of the HH pathway. A thorough functional and biological investigation identified RH2_2 and RH2_6 rhein-based hybrids as valuable candidates for HH inhibition through SMO antagonism, with the consequent suppression of HH-dependent tumour growth. These findings also corroborated the successful application of the NPs-based hybrid design strategy in the development of novel NP-based SMO antagonists.

Introduction

The failure of the large synthetic combinatorial libraries of small molecules represented an important issue of the drug discovery process.[1] Although combinatorial chemistry techniques have succeeded in structural optimization, in the generation of large synthetic compounds libraries, and have been successfully used in the optimization of many recently approved agents, the utilization of natural products (NPs) and/or synthetic variations using their unique structures, to discover and develop the final drug entity, is still alive and well.[2] NPs are highly profitable pharmacological tools due to their chemical diversity and tendency to interact with proteins and modulate biological systems. For example, in the area of cancer, over the time frame from 1946 to 1980, of the 75 small-molecule anticancer drugs, around 53% are NPs or their derivatives (i.e., 40 molecules). However, despite significant progress and several drugs available to treat cancer, the onset of resistance is a major drawback that often causes treatment failure.[3,4] Identifying novel drugs or drug candidates, acting with unexplored and selective mechanisms of action and/or towards novel targets, represents a challenge for anticancer drug discovery and development. In the last decades, targeting specific signalling pathways widely known to be related to the onset and development of tumours has emerged as a great opportunity to develop more effective and less toxic anticancer therapeutic approaches.[4,5] In this field of study, particular interest has been focused on Hedgehog (HH) signalling, a conserved developmental pathway whose aberrant reactivation is responsible for several human cancers, including medulloblastoma (MB) and basal cell carcinoma (BCC), thus emerging as an attractive target for anticancer therapy.[6–12] Extensive efforts were mostly focused on the development of HH modulators acting as antagonists of the upstream G protein-coupled-like receptor SMOOTHENED (SMO).[7] Although some of them have moved into clinical trials

[a] Dr. D. Quaglio,[+] Dr. S. Cammarone, L. Lamelza, Dr. F. Ghirga, L. Pisano, Prof. B. Botta
Department of Chemistry and Technology of Drugs
Sapienza University of Rome
P.le Aldo Moro 5, 00185 Rome (Italy)
E-mail: francesca.ghirga@uniroma1.it

[b] Prof. P. Infante,[+] M. Conenna, G. Adabbo, Prof. L. Di Marcotullio
Department of Molecular Medicine
Sapienza University of Rome
Viale Regina Elena 291, 00161 Rome (Italy)
E-mail: lucia.dimarcotullio@uniroma1.it

[c] Prof. L. Di Marcotullio
Istituto Pasteur-Fondazione Cenci Bolognetti
Sapienza University of Rome
Viale Regina Elena 291, 00161 Rome (Italy)

[d] Prof. M. Mori
Department of Biotechnology, Chemistry and Pharmacy
University of Siena
Via Aldo Moro 2, 53100 Siena (Italy)

[+] These authors contributed equally to this work.

Supporting information for this article is available on the WWW under https://doi.org/10.1002/chem.202302237

This article is part of a joint Special Collection in honor of Maurizio Prato.

for the treatment of HH-dependent tumours and vismodegib, sonidegib, and glasdegib have already been approved by the Food and Drug Administration (FDA) for the treatment of BCC and Acute myelogenous leukemia (AML), respectively, several side effects (i.e., nausea, muscle spasms, and alopecia) and pitfalls, including the onset of SMO drug-resistant mutations, limit their use.[13–17] Currently, one of the most promising strategies to overcome these limitations is the development of second-generation SMO antagonists taking advantage of NPs. Indeed, NPs have played a critical role in understanding HH signalling and its pharmacological modulation, mostly thanks to the steroidal alkaloid cyclopamine, the first inhibitor able to block HH signalling by directly binding to the SMO receptor, identified in the late '90s.[18,19] Indeed, many of the HH inhibitors occur in nature or derive from NPs by means of chemical transformations or total syntheses, which further emphasizes the renewed interest in nature as a source of "hit and lead" compounds in drug discovery.[20] Different design strategies have been utilized to achieve unprecedented and intriguing architectures by intelligently manipulating the NP's core-scaffold.[21–27]

In this context, an alternative approach to discover new biologically relevant compounds, by exploiting the biologically relevant chemical space of NPs, starts from natural chemotypes and employs the combination of the basic skeleton of a NP with a molecularly targeted drug bullet.[28,29] Among the different classes of natural products, anthraquinones, which are secondary metabolites widely distributed in higher plants (aloe, cascara sagrada, senna and rhubarb), microorganisms, lichens and insects, display a wide variability of biological effects.[30] Remarkably, a significant portion of anthraquinone-based drugs approved for clinical practice are antitumour agents.[31] The prominent anthraquinone-based drugs doxorubicin, mitoxantrone, as well as more recent epirubicin, idarubicin, and valrubicin, are successfully used in chemotherapy of haematological malignancies and solid tumours.[32] The anthraquinone core remains a promising scaffold for discovering novel drug candidates.[30,31,33,34]

Based on these findings, this work provides an innovative exploitation of the chemical versatility as well as the affinity for the HH pathway of the anthraquinone scaffold by combining it with the active portion of well-known SMO antagonists (Taladegib and Anta XV) to design, synthesize and test specific antagonists. Our strategy implied the design, supported by computer-aided methods, and synthesis of a library of anthraquinone derivatives featuring variously substituted piperazine linkers, able to interact in silico with the SMO receptor, and the investigation of the HH inhibitory properties of the synthesized compounds, to validate the computational modelling predictions.

This study offers an alternative approach to turn natural products from nontargeted to targeted anticancer therapies by exploiting natural sources and combining them with modern technologies for guided lead identification and synthesis/development.

Results and Discussion

First generation of anthraquinone-like SMO antagonists: Hit identification

To discover new potent SMO-targeting antagonists, the naturally-occurring anthraquinone structure was selected as a promising scaffold based on its chemical features and versatility besides its wide distribution in nature.[28,35] From a chemical standpoint, anthraquinones are a group of polyketides of the quinone family with a basic cyclic scaffold composed of three fused benzene rings, including two ketone groups on the central 9,10-carbons. The rigidity, planarity, and aromaticity of the anthraquinone system have been widely studied with respect to its pharmacological properties. Indeed, anthraquinones have attracted chemists' interest in accessing diversely substituted derivatives via different synthetic protocols. Although several synthetic approaches are available to synthesize substituted anthraquinones, most of the derivatives have been prepared via efficient semi-synthetic approaches starting from commercially available compounds in recent years. Herein, due to the easy accessibility to plant sources, low commercial cost, and structural features, emodin (1,3,8-trihydroxy-6-methylanthraquinone) was identified as an ideal candidate for the preparation of a novel generation of SMO antagonists by exploring hybrid scaffold design approach.[36] Therefore, a small-focused library of anthraquinone derivatives, EP1-EP22 (Figure S1), was rationally designed by combining the basic skeleton of emodin with piperazine or piperidine nuclei structurally similar to the SMO-targeting bullet of well-established SMO antagonists (Taladegib and Anta XV) (Figure 1).

Moreover, the methylene connection between the C-2 position of emodin and piperazine or piperidine linkers variously substituted was conceived based on a facile multicomponent Mannich-type reaction procedure. The binding mode and theoretical affinity of the emodin derivatives were evaluated by molecular docking with the FRED program from OpenEye, Cadence Molecular Sciences, using the settings and protocols already refined and validated in previous works.[37–39] The outcomes of this initial molecular docking investigation showed that all designed molecules bind in an improper orientation toward the SMO antagonists' site. Indeed, the sp^3 hybridization of the nitrogen atoms of the piperazine or piperidine portion linked via a methylene bridge to the C-2 position of the anthraquinone core favours its protonation at physiological pH values (i.e., pH = 7.4), thus hindering the interaction within the deepest portion of the SMO binding site (data not shown), which is targeted by the anthraquinone core. In order to overcome these structural issues, the related anthraquinone metabolite rhein (1,8-dihydroxyanthraquinone 3-carboxylic acid), featuring an easily functionalizable acid group at C-3 position, was exploited as an alternative scaffold. Therefore, a small-size focused library of rhein derivatives was rationally designed to further reduce the polarity of the anthraquinone scaffold by methylating hydroxyl groups, and to avoid the nitrogen protonation at pH 7.4 by linking the standard SMO-targeting bullet of Anta XV with rhein (Figure 2)

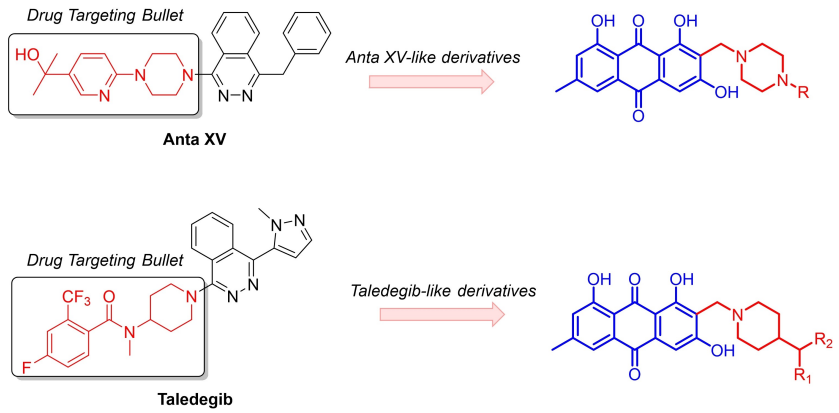

Figure 1. Rational design of emodin derivatives as potential SMO antagonists.

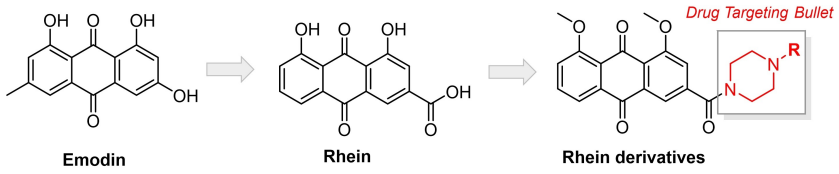

Figure 2. Rational design of rhein derivatives as potential SMO antagonists.

via an amide bond formation. In this case, missing the nitrogen basic properties, the protonation at pH 7.4 should be prevented, thus favouring the correct orientation of the molecule inside the binding pocket of the SMO receptor.

As a result, the series RH1-RH6 (Figure S2) was conceived and enhanced upon the previous EP1-EP22 series. Notably, docking studies revealed that molecules of this small-focused library of naturally-inspired compounds share a highly similar binding mode within the antagonists site of the SMO receptor. Specifically, molecular docking highlighted four compounds (RH1-RH4) favourable binding poses and best scores at the receptor site. The large and flat anthraquinone moiety binds near the entrance of the binding site within the region of the receptor that is located in proximity to the outer side of the membrane (Figure 3A). Here, hydrogen-bond interactions with Asn219, Tyr394 and Gln477 are established. In contrast, the variable portion of the molecules binds in the inner and narrow region of the receptor where it stacks to the side chain of Phe391 (Figure 3A). Finally, a good overlapping with the binding mode of crystallographic ligand Anta XV is observed (Figure 3B). Based on these findings, rhein-based derivatives, RH1-RH4, were selected for organic synthesis and functional evaluation.

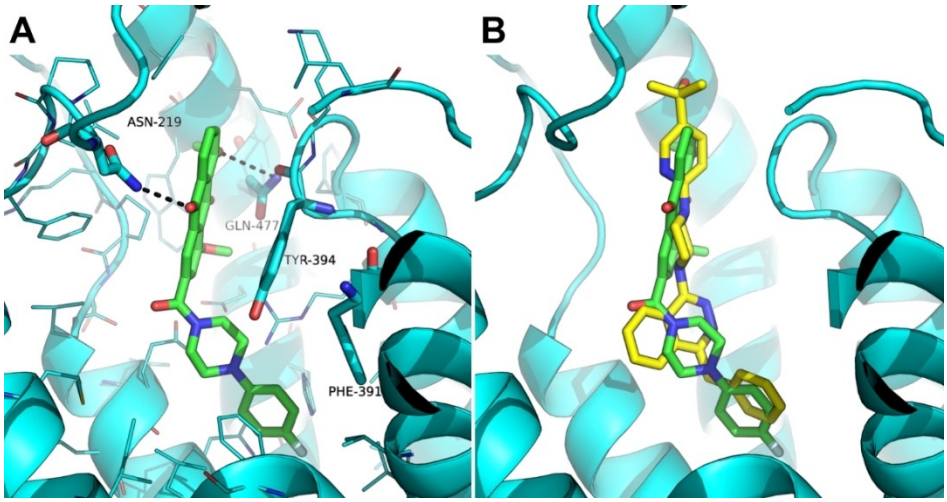

Figure 3. Predicted binding mode of RH2 to SMO. **A**) Docking pose of RH2 is shown as green sticks, the X-ray crystallographic structure of SMO coded by PDB-ID: 4JKV is shown as cyan cartoon and lines (residues within 5 Å from the ligand are shown, others are hidden), H-bonds are highlighted by black dashed lines. **B**) structural overlapping between the crystallized *Smo* antagonist, Anta XV (yellow sticks), and RH2 (green sticks).

A convergent synthetic strategy, involving Steglich-like coupling of the dimethyl rhein with variously substituted piperazines, has been considered the most suitable approach for the preparation of RH1-RH4 (Scheme 1). Starting from commercially available rhein (**1**), the methylation of the anthraquinone hydroxyl and carboxylic acid groups was performed using methyl iodide (CH_3I) in the presence of NaH as base affording **2** in quantitative yield. To allow the further condensation reaction, the methyl ester functionality of **2** was hydrolysed by using a basic solution of NaOH (1 M) in ethanol/water (1:1, v/v) followed by an acid solution of HCl (1 M) to obtain the corresponding carboxylic acid derivative **3** in 87% yield. The further step consisted in the Steglich-type amidation of **3** with the corresponding piperazine linkers featuring phenyl/pyridine/pyrimidine moieties at position 4.

The reaction was performed under mild conditions by employing the coupling reagent EDCI, a water-soluble derivative of carbodiimide, in the presence of DMAP: commercially available amino linkers, i.e., 1-phenylpiperazine and 1-(4-fluorophenyl)-piperazine, were employed for the synthesis of RH1 (43% yield) and RH2 (46% yield) derivatives; 2-(6-(piperazin-1-yl)pyridin-3-yl)propan-2-ol and 2-(5-(piperazin-1-yl)pyrazin-2-yl)propan-2-ol linkers were synthesized according to previously developed procedures and used for the preparation of RH3 (50% yield) and RH4 (60% yield), respectively (Scheme S1).[40]

The HH inhibitory properties of the synthesized compounds, RH1-RH4, were investigated in a luciferase reporter assay, which is widely used for characterizing HH antagonists.[36] To this end, NIH3T3 SHH-Light II cells stably incorporating a Gli-responsive firefly luciferase reporter (Gli-RE) and the pRL-TK Renilla as normalization control, were treated with the synthetic SMO agonist (SAG) alone or in combination with the selected molecules. Among the tested compounds only RH2 showed inhibitory activity with an IC_{50} of 5.698 μM (Figure 4), whereas RH1 was inactive (Figure 4) and RH3 and RH4 showed unspecific effect due to the modulation of the internal normalization control (Figure S3).

Second generation of anthraquinone-like SMO antagonists: Hit optimization

The iterative cycle of design-synthesis-testing was implemented to accelerate the optimization of chemical structures with respect to HH inhibition. Therefore, the most promising compound RH2, featuring a piperazine linker substituted at position 4 with a *p*-fluorophenyl group, emerged from the

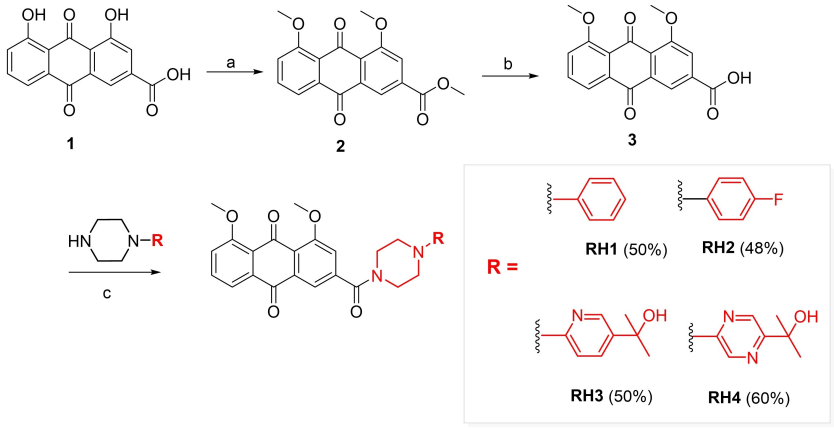

Scheme 1. Synthesis of rhein-amides (**RH1-RH4**). Reagents and conditions: a) NaH, CH_3I, dry CH_2Cl_2, N_2, 0 °C to rt, o/n, quantitative. b) 1) NaOH, EtOH, 50 °C, 2.5 h; 2) HCl, 0 °C, 87%; c) EDCI, DMAP, dry CH_2Cl_2, 0 °C to rt, o/n.

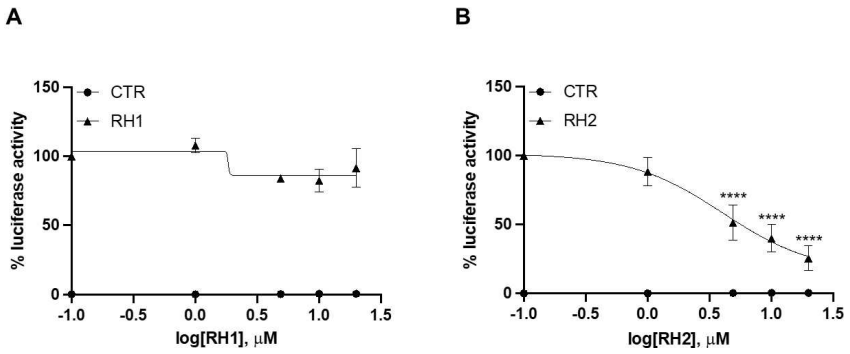

Figure 4. Inhibitory effect of RH compounds on HH signaling activity. Dose-response curve of compounds **RH1** (**A**) and **RH2** (**B**) in SAG-treated NIH3T3 Shh Light II cells. Treatment time was 48 h and data were normalized against Renilla luciferase. Data show the mean ± SD of three independent experiments. (****) $p < 0.0001$ vs SAG.

functional evaluation of the first generation of rhein-based derivatives, and it was used as a privileged hit compound towards this aim. A second generation of anthraquinone-like SMO antagonists, RH2_1-RH2_9, was rationally designed by modifying the p-fluoro substitution on the phenyl group, the region of the scaffold responsible for the selective antagonism of SMO, with several functional groups. In particular, in RH2_1-RH2_6, the phenyl group linked to the piperazine nucleus shows different substituents at para position, while in RH2_7-RH2-9, the phenyl group is substituted with a pyridine group in which the nitrogen atom is in the 2- (RH2_7), 3- (RH2_8) or 4- (RH2_9) position, respectively (Figure S4). The second generation of anthraquinone-like derivatives was tested in silico to evaluate the binding mode and theoretical affinity towards the crystallographic structure of SMO. Based on a combination of visual inspection of binding modes and analysis of docking score, compounds RH2_3, RH2_4, RH2_5 and RH2_6 resulted the most interesting of the series (Figure S5) since they appear to be even more effective than the parent RH2, whereas other compounds proved less effective than, or at least comparable to, RH2. Accordingly, all the derivatives of this series were selected for organic synthesis and biological studies.

The synthetic strategy used for obtaining the second series of RHs compounds is the same one previously discussed (Scheme 1) and involves the same reactions. Notably, it has been found that the second series was more advantageous compared to the previous one, which required the synthesis of some piperazine linkers for RH3 and RH4, before being linked to the anthraquinone core of rhein (Scheme 2). As a matter of fact, the piperazine linkers (**13**-**21**) used for obtaining RH2_1-RH2_9 are all readily available in commerce and are reasonably cheap (Scheme 2).

The RH2_1-RH2_9 derivatives have been tested in a range from 1 to 50 μM for their ability to suppress HH signalling by luciferase reporter assays in NIH3T3 SHH-Light II cells as described above (Figure 5).[41] Among them, RH2_3 and RH2_9 showed unspecific effect due to the modulation of the internal normalization control TK-Renilla (Figure S6), whereas the derivatives RH2_2 and RH2_6 emerged as the most active, with an IC_{50} value of 1.585 and 1.658 μM, respectively (Figure 5B,E). Notably, electron-donating groups proved more effective than the electron-withdrawing group substituted to the phenyl ring connected to the rhein core by the piperazine linker. The effect of RH2_2 and RH2_6 to inhibit the HH pathway was confirmed in *Ptch1*$^{-/-}$ mouse embryonic fibroblasts (MEFs), in which the constitutive activation of HH signalling is the consequence of the loss of repressive receptor *Ptch1* gene.[41]

As shown in Figure 6A, RH2_2 and RH2_6 significantly reduced mRNA expression levels of HH target genes (i.e., *Gli1*, *Gli2*, and *CycD1*). Conversely, in cells lacking the Smo receptor (*Smo*$^{-/-}$ MEFs), both compounds, as well as the well-known SMO antagonist vismodegib, did not affect the mRNA levels of *Gli1*, the final and the most powerful effector of HH signalling (Figure 6B). It is worth noting that although in *Smo*$^{-/-}$ MEFs the levels of the *Gli1* mRNA are lower than wildtype cells, the RNA levels are detectable and can be pharmacologically modulated.[37] These results indicate the specificity of RH2_2 and RH2_6 as SMO antagonists. Finally, we tested the inhibitory effect of RH2_2 and RH2_6 on HH-dependent medulloblastoma (MB) cell models, since the strong correlation between the aberrant activation of HH signalling and the onset of this malignant brain tumour.

To this aim, we used Med1-MB cell line derived from a spontaneous tumour arisen in a *Ptch1*$^{+/-}$,*lacZ* mouse and primary MB cells freshly isolated from Math1-cre/Ptch$^{-/-}$ mice that spontaneously develop MB.[42,43] As shown in Figures 7A and C both the compounds suppressed the proliferation of MB cells over time and this effect correlated as expected with the reduction of the expression levels of HH target genes, such as *Gli1*, *Gli2*, and *CycD1* (Figure 7B, D). These findings reveal the compounds RH2_2 and RH2_6 as good candidates for the inhibition of HH signalling by acting on Smo with the consequent suppression of HH-dependent tumour growth.

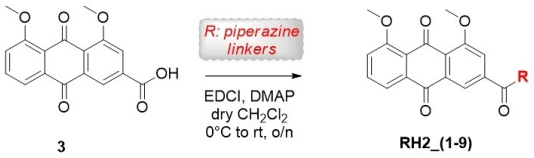

Cmpd. (yield %)	R:	Cmpd.	R:	Cmpd.	R:
RH2_1 (53%)	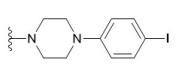	**RH2_4** (50%)	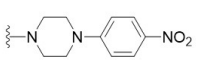	**RH2_7** (64%)	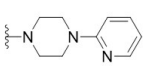
RH2_2 (40%)	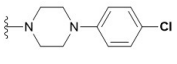	**RH2_5** (50%)	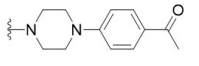	**RH2_8** (68%)	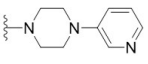
RH2_3 (60%)	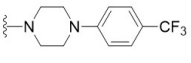	**RH2_6** (88%)	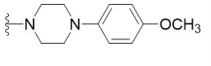	**RH2_9** (70%)	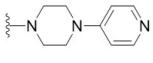

Scheme 2. Synthesis of novel **RHs** derivatives using different piperazine linkers.

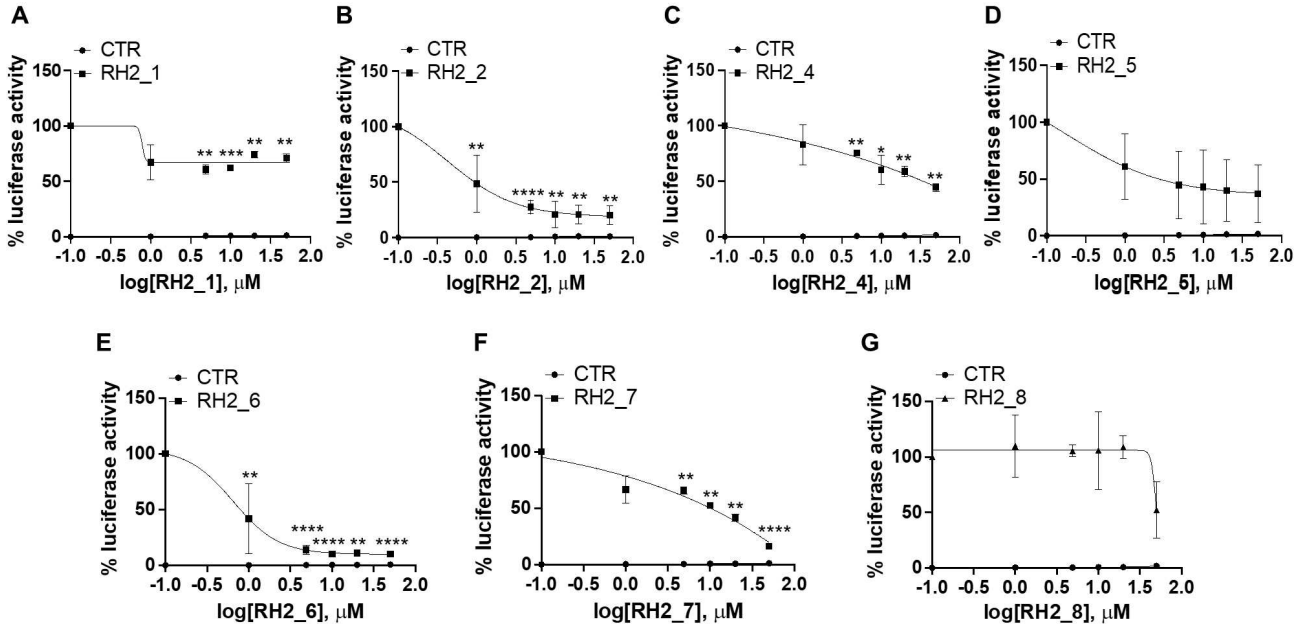

Figure 5. Inhibitory effect of RH2 derivatives on HH signaling activity. Dose-response curves of RH2 derivatives in SAG-treated NIH3T3 Shh Light II cells. Treatment time was 48 h and data were normalized against Renilla luciferase. Data show the mean ± SD of three independent experiments. (*) $p < 0.05$; (**) $p < 0.01$; (***) $p < 0.001$; (****) $p < 0.0001$ vs SAG.

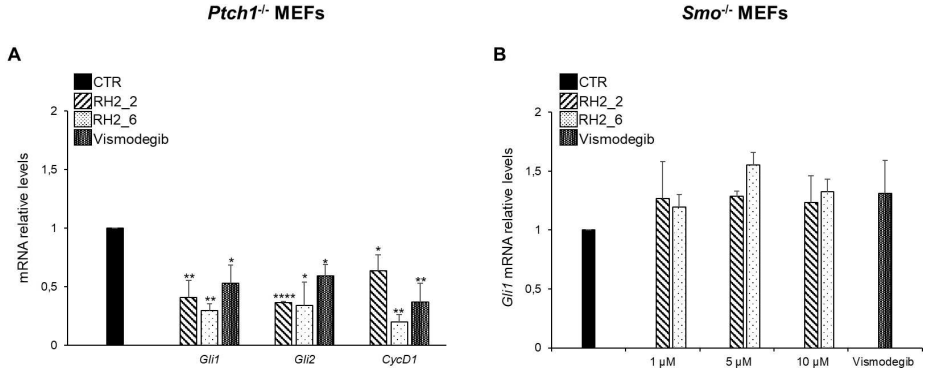

Figure 6. The effect of RH2_2 and RH2_6 in HH-dependent cell models**. (A)** The graph shows the mRNA expression levels of HH target genes (i.e., *Gli1*, *Gli2*, and *CycD1*) in *Ptch1*$^{-/-}$ MEFs treated for 48 h with DMSO as a control, or **RH2_2**, or **RH2_6** at the final concentration of 1 μM, or Vismodegib (100 nM). **(B)** The graph shows the mRNA expression levels of *Gli1* in *Smo*$^{-/-}$ MEFs treated for 48 h with DMSO as a control, or **RH2_2**, or **RH2_6** at the final concentrations of 1, 5, 10 μM, or Vismodegib (100 nM), used as control. All data show the mean ± SD of three independent experiments normalized to endogenous controls *β2-microglobulin* and *Hprt*. (*) $p < 0.05$; (**); $p < 0.01$; (****); $p < 0.0001$ vs CTR.

Conclusions

In conclusion, a new design principle to turn NPs from nontargeted to targeted SMO antagonists was explored. The combination of the emodin-like scaffold (i.e., rhein) with the active portion of such well-established and known SMO antagonists (Taladegib and Anta XV) resulted in a collection of anthraquinone-based hybrids acting as SMO antagonists. An iterative drug discovery process was conceived to accelerate the evaluation and optimization of chemical structure in silico ahead of synthesis and assay. Therefore, a small-focused library of anthraquinone-based hybrids, RH1-RH4, was rationally designed by combining the basic skeleton of rhein with variously substituted piperazine nuclei structurally similar to the SMO-targeting bullets. The most promising compound RH2, featuring a piperazine linker substituted in position 4 with a *p*-fluorophenyl group, emerged from the functional evaluation and was further optimized through an additional cycle of design-synthesis-bioassay and testing in vitro. Among the second generation of rhein-based derivatives, RH2_2 and RH2_6, featuring a *p*-chloro and a *p*-methoxy substitution on the phenyl group, respectively, emerged as the most effective in inhibiting the HH signalling activity. Further, a thorough functional and biological characterization of the most potent hybrids, RH2_2 and RH2_6, revealed them as good candidates for the inhibition of the HH pathway by acting on SMO with the consequent block of HH-dependent tumour growth. Therefore, the results highlight the successful application of the NPs-based hybrid design strategy for developing novel generations of SMO antagonists and expand the repertoire of chemotypes for

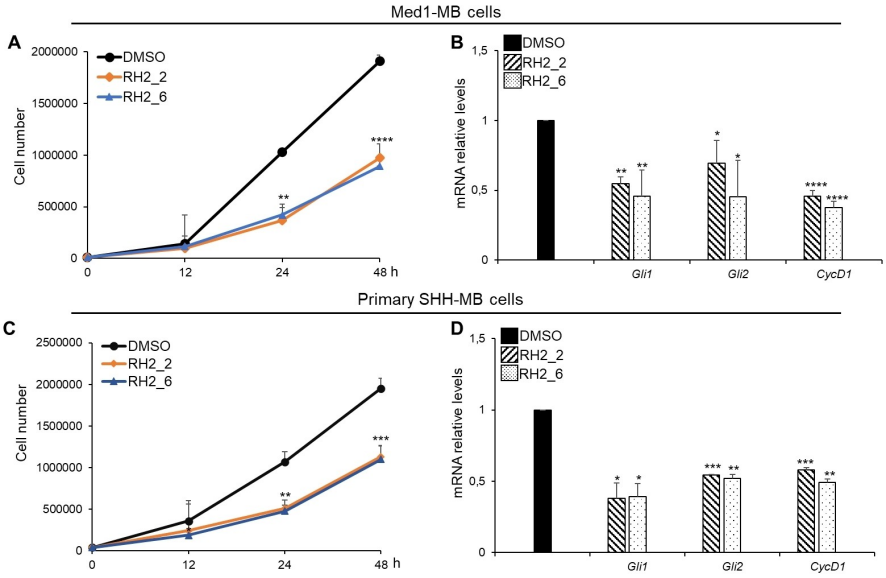

Figure 7. Tumor growth inhibition of SHH-MB cells in vitro by RH2_2 and RH2_6. **(A, C)** Med1-MB cells and primary murine SHH-MB cells freshly isolated from Math1-cre/Ptch$^{-/-}$ mice were treated with RH2_2 or RH2_6 at the final concentration of 1 μM, or DMSO only. After the indicated times, a trypan blue count was performed to determine the growth rate of viable cells. **(B, D)** The relative expression levels HH target genes (i.e., *Gli1*, *Gli2*, and *CycD1*) have been evaluated by qRT–PCR in SHH cell models treated with RH2_2 and RH2_6 (1 μM), or DMSO only. Data show the mean ± SD of three independent normalized to endogenous controls *β2-microglobulin* and *Hprt*. (*) $p < 0.05$ vs DMSO; (**) $p < 0.01$ vs DMSO; (***) $p < 0.001$; (****) $p < 0.0001$ vs DMSO.

SMO inhibition by exploring the biologically relevant chemical space NPs and making them targeted compounds.

Material and Methods

General procedure for the synthesis of rhein amide derivatives through a Steglich amidation

To a stirring solution of carboxylic acid **3** (150 mg, 0.48 mmol, 1 equiv.) in dry CH_2Cl_2 (20 mL), EDCI·HCl (115 mg, 0.60 mmol, 1.25 equiv.) and DMAP (59 mg, 0.48 mmol, 1 equiv.) were added at 0 °C under inert atmosphere. After 5 min, the desired piperazine derivative (commercially available linkers 1-phenyl-piperazine, 1-(4-fluorophenyl)-piperazine and **13**–**21**) (0.96 mmol, 2 equiv.) was added. The reaction mixture was warmed up to room temperature and stirred overnight. The mixture was then quenched with water, extracted with CH_2Cl_2 (3 x 20 mL), washed with brine, dried over Na_2SO_4, filtered and concentrated in vacuo. The residues obtained were further purified according to the procedures discussed in the Supporting Information.

Cell cultures and treatments

NIH3T3 Shh-Light II, *Ptch1*$^{-/-}$ (kindly provided by M.P. Scott), *Smo*$^{-/-}$ (kindly provided by R. Toftgard), Med1-MB cells (kindly provided by Yoon-Jae Cho) were cultured in Dulbecco's Modified Eagle Medium (DMEM) (Euroclone, Milan, Italy) supplemented with 10% fetal bovine serum (FBS; Sigma-Aldrich St. Louis, MO, USA). All media contained 1% L-Glutamine and 1% Penicillin–Streptomycin (Pen/Strep).

Primary MB cells were freshly isolated from Math1-cre/Ptch$^{-/-}$ mice. Tumours were collected and mechanically disgregated in HBSS plus 1% Pen/Strep using sterilized Pasteur pipettes. The samples were treated with DNase (10 μg/mL) for twenty minutes to obtain a single-cell suspension. Finally, cells were centrifuged and resuspended in Neurobasal Media-A with B27 supplement minus vitamin A, 1% Pen/Strep and 1% L-glutamine and freshly used for in vitro proliferation assays.

Mycoplasma contamination in cell cultures was routinely detected using PCR detection kit (Applied Biological Materials, Richmond, BC, Canada).

NIH3T3 Shh-Light II cells were treated with the tested compounds (at the indicated concentrations) and SAG (200 nM, Alexis Biochemicals Farmingdale, NY, USA) for 48 h. *Smo*$^{-/-}$ and *Ptch1*$^{-/-}$ MEFs were treated with the tested compounds, at the indicated concentrations, for 48 h, respectively. Where indicated, cells were treated with Vismodegib (100 nM, Selleckchem) used as control.

Molecular modelling

Docking simulations were carried out with FRED (OpenEye, Cadence Molecular Sciences) version 3.3.0.3[44–47] using the crystallographic structure of the SMO coded by PDB-ID: 4JKV as a rigid receptor (chain A).[48]

Before docking, co-crystallized ligands were removed. The receptor binding site was defined within the SMO heptahelical bundle, where co-crystalized SMO antagonists are found by X-ray crystallography. Ligands were sketched in Picto (OpenEye,

Cadence Molecular Sciences and then converted into three-dimensional structures with OMEGA (OpenEye, Cadence Molecular Sciences) version 3.1.0.3.[49–51] By molecular docking with FRED, 5 top- scoring poses of each ligand were stored and submitted to visual inspection.

Luciferase reporter assay

Luciferase reporter assay has been performed in NIH3T3 Shh-Light II cells, stably expressing a Gli-responsive luciferase reporter and the pRL-TK Renilla (normalization control). NIH3T3 Shh-Light II cells were seeded into 24-well cell culture plates and maintained in culture for three days to achieve optimal cell confluence (about 90%) for SAG treatment. Cells were then treated for 48 h with SAG (200 nM) alone or in combination with the tested compounds at the indicated concentrations. According to the manufacturer's instructions, Luciferase and Renilla activities were assayed with a dual-luciferase assay system (Biotium Inc., Hayward, CA, USA). Results were expressed as Luciferase/Renilla ratios and represented the mean ± S.D. of three experiments performed in triplicate.

Proliferation assay

The proliferation of Med1-MB and primary SHH-MB cells was evaluated by a trypan blue count after a treatment period of 12, 24, and 48 h with the compounds of interest, or solvent (DMSO) only used as control. Briefly, Med1-MB cells and SHH-MB primary cells were seeded in 24-well cell culture plates to obtain a starting cell density of 10^4 cells/well and 40^4 cells/well, respectively. Then, the cells were treated with the compounds of interest, or DMSO only used as vehicle. After 12, 24 and 48 h of treatment, the proliferation rate of viable cells was assessed by trypan blue staining. Results represent the mean ± S.D. of three experiments performed in triplicate.

mRNA Expression analysis

Trizol reagent (Invitrogen/Life Technologies) was used to isolate total RNA from cells and reverse transcribed with SensiFAST cDNA Synthesis Kit (Bioline Reagents Limited, London, UK). Quantitative real-time PCR (Q-PCR) analysis of *Gli1*, *Gli2*, *Cyclin D1*, *β2-microglobulin, and Hprt* mRNA expression was performed by using the VIIA7 Real Time PCR System (Life Technologies). Standard Q-PCR thermal cycler parameters were used to amplify a reaction mixture containing cDNA template, SensiFAST SYBR Lo-ROX Kit (Bioline Reagents Limited) and primer probe. Each amplification reaction was performed in triplicate, and the average of the three threshold cycles was used to calculate the amount of transcript in the sample by using SDS version 2.3 software. Data were normalized with the endogenous housekeeping genes (*β2-microglobulin* and *Hprt*) and expressed as the fold change respect to the control sample value.

Statistical analysis

Results are expressed as mean ± S.D. from an appropriate number of experiments (at least three biological replicas). For all other experiments, p values were determined using two-tailed Student's t-test, and statistical significance was set at $p < 0.05$.

Acknowledgements

This work was supported Ministry of University and Research (PRIN 2017BF3PXZ003), Progetti di Ricerca di Università Sapienza di Roma, Universities and Research-Dipartimenti di Eccellenza-L.232/2016, Pasteur Institute/Cenci Bolognetti Foundation, and AIRC (Associazione Italiana per la Ricerca sul Cancro) #IG20801 to LDM, and MFAG 2021-ID. 26536 to PI. G. Adabbo is the recipient of a fellowship of the PhD Programme in Molecular Medicine, University La Sapienza, Rome, Italy, supported by NextGenerationEU" DD. 3175/2021 E DD. 3138/2021. CN_3: National Center for Gene Therapy and Drugs based on RNA Technology Codice Progetto CN 00000041. MM wish to thank the OpenEye Free Academic Licensing Programme for providing a free academic licence for molecular modeling and chemoinformatics software.

Conflict of Interests

The authors declare no conflict of interest.

Data Availability Statement

The data that support the findings of this study are available from the corresponding author upon reasonable request.

Keywords: anthraquinones · Hedgehog pathway · hybrid compounds · natural products · SMO antagonists

[1] A. G. Atanasov, S. B. Zotchev, V. M. Dirsch, C. T. Supuran, *Nat. Rev. Drug Discovery* **2021**, *20 (3)*, 200–216.
[2] D. J. Newman, G. M. Cragg, *J. Nat. Prod.* **2020**, *83 (3)*, 770–803.
[3] https://gco.iarc.fr/today/data/factsheets/populations/900-world-fact-sheets.pdf.
[4] Y. Li, Z. Wang, J. A. Ajani, S. Song, *Cell Commun. Signaling* **2021**, *19 (1)*, 19.
[5] J. D. Ebben, D. M. Treisman, M. Zorniak, R. G. Kutty, P. A. Clark, J. S. Kuo, *Expert Opin. Ther. Targets* **2010**, *14 (6)*, 621–632.
[6] C. Bichakjian, A. Armstrong, C. Baum, J. S. Bordeaux, M. Brown, K. J. Busam, D. B. Eisen, V. Iyengar, C. Lober, D. J. J. J. o. t. A. A. o. D. Margolis, *Journal of the American Academy of Dermatology* **2018**, *78 (3)*, 540–559.
[7] F. Ghirga, M. Mori, P. J. Infante, *Bioorg. Med. Chem. Lett.* **2018**, *28 (19)*, 3131–3140.
[8] D. Girardi, A. Barrichello, G. Fernandes, A. Pereira, *Cells* **2019**, *8 (2)*, 153.
[9] P. Infante, R. Faedda, F. Bernardi, F. Bufalieri, L. Lospinoso Severini, R. Alfonsi, D. Mazzà, M. Siler, S. Coni, A. Po, *Nat. Commun.* **2018**, *9 (1)*, 976.
[10] L. Lospinoso Severini, F. Ghirga, F. Bufalieri, D. Quaglio, P. Infante, L. Di Marcotullio, *Expert Opin. Ther. Targets* **2020**, *24 (11)*, 1159–1181.

[11] P. A. Northcott, G. W. Robinson, C. P. Kratz, D. J. Mabbott, S. L. Pomeroy, S. C. Clifford, S. Rutkowski, D. W. Ellison, D. Malkin, M. D. Taylor, A. Gajjar, S. M. Pfister, *Nat. Rev. Dis. Primers* **2019**, *5 (1)*, 11.
[12] D. Quaglio, P. Infante, L. Di Marcotullio, B. Botta, M. Mori, *Expert Opin. Ther. Pat.* **2020**, *30 (4)*, 235–250.
[13] S. X. Atwood, K. Y. Sarin, R. J. Whitson, J. R. Li, G. Kim, M. Rezaee, M. S. Ally, J. Kim, C. Yao, A. L. S. Chang, A. E. Oro, J. Y. Tang, *Cancer Cell* **2015**, *27 (3)*, 342–353.
[14] C. Danial, K. Y. Sarin, A. E. Oro, A. L. S. Chang, *Clin. Cancer Res.* **2016**, *22 (6)*, 1325–1329.
[15] J. George, Y. Chen, N. Abdelfattah, K. Yamamoto, T. D. Gallup, S. I. Adamson, B. Rybinski, A. Srivastava, P. Kumar, M. G. Lee, *Cancer Res. Commun.* **2022**, *2 (6)*, 402–416.
[16] H. Q. Doan, L. Chen, Z. Nawas, H.-H. Lee, S. Silapunt, M. Migden, *Oncotarget* **2021**, *12 (20)*, 2089.
[17] N. M. Nguyen, J. Cho, *Int. J. Molec. Sci.* **2022**, *23 (3)*, 1733.
[18] J. K. Chen, *Nat. Prod. Rep.* **2016**, *33 (5)*, 595–601.
[19] R. Palermo, F. Ghirga, M. G. Piccioni, F. Bernardi, N. Zhdanovskaya, P. Infante, M. Mori, *Curr. Pharm. Des.* **2018**, *24 (36)*, 4251–4269.
[20] C. Bao, P. Kramata, H. J. Lee, N. J. Suh, *Mol. Nutr. Food Res.* **2018**, *62 (1)*, 1700621.
[21] E. A. Crane, K. Gademann, *Angew. Chem. Int. Ed.* **2016**, *55 (12)*, 3882–3902.
[22] G. S. Cremosnik, J. Liu, H. Waldmann, *Nat. Prod. Rep.* **2020**, *37 (11)*, 1497–1510.
[23] M. Grigalunas, S. Patil, A. Krzyzanowski, A. Pahl, J. Flegel, B. Schölermann, J. Xie, S. Sievers, S. Ziegler, H. Waldmann, *Chem. Eur. J.* **2022**, *28 (67)*, e202202164.
[24] G. Karageorgis, D. J. Foley, L. Laraia, H. Waldmann, *Nat. Chem.* **2020**, *12 (3)*, 227–235.
[25] L. Laraia, G. Garivet, D. J. Foley, N. Kaiser, S. Müller, S. Zinken, T. Pinkert, J. Wilke, D. Corkery, A. Pahl, *Angew. Chem. Int. Ed.* **2020**, *59 (14)*, 5721–5729.
[26] K. C. Morrison, P. J. Hergenrother, *Nat. Prod. Rep.* **2013**, *31 (1)*, 6–14.
[27] S. Wetzel, R. S. Bon, K. Kumar, H. Waldmann, *Angew. Chem. Int. Ed.* **2011**, *50 (46)*, 10800–10826.
[28] G. Liu, D. Xue, J. Yang, J. Wang, X. Liu, W. Huang, J. Li, Y.-Q. Long, W. Tan, A. Zhang, *J. Med. Chem.* **2016**, *59 (24)*, 11050–11068.
[29] E. Sflakidou, G. Leonidis, E. Foroglou, C. Siokatas, V. Sarli, *Molecules* **2022**, *27 (19)*, 6632.
[30] E. M. Malik, C. E. Müller, *Med. Res. Rev.* **2016**, *36 (4)*, 705–748.
[31] T. Narender, P. Sukanya, K. Sharma, S. R. Bathula, *Phytomedicine* **2013**, *20 (10)*, 890–896.
[32] A. S. Tikhomirov, A. A. Shtil, A. E. Shchekotikhin, *Recent Pat. Anti-Infect. Drug Discovery* **2018**, *13 (2)*, 159–183.
[33] S. Ciaco, V. Mazzoleni, A. Javed, S. Eiler, M. Ruff, M. Mousli, M. Mori, Y. Mély, *Bioorg. Chem.* **2023**, *137*, 106616.
[34] L. Zaayter, M. Mori, T. Ahmad, W. Ashraf, C. Boudier, V. Kilin, K. Gavvala, L. Richert, S. Eiler, M. Ruff, M. Botta, C. Bronner, M. Mousli, Y. Mély, *Chem. Eur. J.* **2019**, *25 (58)*, 13363–13375.
[35] M. Sebak, F. Molham, C. Greco, M. A. Tammam, M. Sobeh, A. El-Demerdash, *RSC Adv.* **2022**, *12 (38)*, 24887–24921.
[36] R. B. Semwal, D. K. Semwal, S. Combrinck, A. Viljoen, *Phytochemistry* **2021**, *190*, 112854.
[37] L. Lospinoso Severini, D. Quaglio, I. Basili, F. Ghirga, F. Bufalieri, M. Caimano, S. Balducci, M. Moretti, I. Romeo, E. Loricchio, *Cancers* **2019**, *11 (10)*, 1518.
[38] S. Berardozzi, F. Bernardi, P. Infante, C. Ingallina, S. Toscano, E. De Paolis, R. Alfonsi, M. Caimano, B. Botta, M. Mori, L. Di Marcotullio, F. Ghirga, *Eur. J. Med. Chem.* **2018**, *156*, 554–562.
[39] R. Alfonsi, B. Botta, S. Cacchi, L. Di Marcotullio, G. Fabrizi, R. Faedda, A. Goggiamani, A. Iazzetti, M. Mori, *J. Med. Chem.* **2017**, *60 (4)*, 1469–1477.
[40] PCT/CN2015/074268, Q. D. A. S. I..
[41] J. Taipale, J. K. Chen, M. K. Cooper, B. Wang, R. K. Mann, L. Milenkovic, M. P. Scott, P. A. Beachy, *Nat. Chem.* **2000**, *406 (6799)*, 1005–1009.
[42] M. G. Hayden Gephart, Y. S. Su, S. Bandara, F.-C. Tsai, J. Hong, N. Conley, H. Rayburn, L. Milenkovic, T. Meyer, M. P. Scott, *J. Neuro-Oncol.* **2013**, *115*, 161–168.
[43] Z.-J. Yang, T. Ellis, S. L. Markant, T.-A. Read, J. D. Kessler, M. Bourboulas, U. Schüller, R. Machold, G. Fishell, D. H. Rowitch, *Cancer Cell* **2008**, *14 (2)*, 135–145.
[44] FRED 3.3.0.3. OpenEye, C. M. S., Inc., Santa Fe, NM. http://www.eyesopen.com.
[45] B. P. Kelley, S. P. Brown, G. L. Warren, S. W. Muchmore, *J. Chem. Inf. Model.* **2015**, *55 (8)*, 1771–1780.
[46] M. McGann, *J. Chem. Inf. Model.* **2011**, *51 (3)*, 578–596.
[47] M. McGann, *J. Comput.-Aided Mol. Des.* **2012**, *26 (8)*, 897–906.
[48] C. Wang, H. Wu, V. Katritch, G. W. Han, X.-P. Huang, W. Liu, F. Y. Siu, B. L. Roth, V. Cherezov, R. C. Stevens, *Nat. Chem.* **2013**, *497 (7449)*, 338–343.
[49] P. C. Hawkins, A. G. Skillman, G. L. Warren, B. A. Ellingson, M. T. Stahl, *J. Chem. Inf. Model.* **2010**, *50 (4)*, 572–584.
[50] OMEGA 3.1.0.3. OpenEye, C. M. S., Santa Fe, NM. http://www.eyesopen.com.
[51] VIDA 4.4.0.4 OpenEye, C. M. S., Santa Fe, NM http://www.eyesopen.com.

Manuscript received: July 13, 2023
Accepted manuscript online: August 10, 2023
Version of record online: September 25, 2023